Investigation of FPGA Based Real Time Adaptive Digital Pulse Shaping for High Count Rate Applications

Shefali Saxena, and Ayman I. Hawari

***Abstract*— Digital signal processing techniques have been widely used in radiation spectrometry to provide improved stability and performance with compact physical size over the traditional analog signal processing. In this work, field programmable gate array (FPGA) based adaptive digital pulse shaping techniques are investigated for real-time signal processing. National Instruments (NI) NI 5761 14 bit, 250 MS/s adaptor module is used for digitizing high purity germanium (HPGe) detector's preamplifier pulses. Digital pulse processing algorithms are implemented on the NI PXIe-7975R reconfigurable FPGA (Kintex-7) using the LabVIEW FPGA module. Based on the time separation between successive input pulses, the adaptive shaping algorithm selects the optimum shaping parameters (rise time and flattop time of trapezoid shaping filter) for each incoming signal. A digital Sallen-Key low pass filter is implemented to enhance signal to noise ratio and reduce baseline drifting in trapezoid shaping. A recursive trapezoid shaping filter algorithm is employed for pole-zero compensation of exponentially decayed (with two decay constants) preamplifier pulses of an HPGe detector. It allows extraction of pulse height information at the beginning of each pulse, thereby reducing the pulse pile up and increasing throughput. The algorithms for RC-CR^2 timing filter, baseline restoration, pile-up rejection and pulse height determination are digitally implemented for radiation spectroscopy. Traditionally, at high-count rate conditions, a shorter shaping time is preferred to achieve high throughput, which deteriorates energy resolution. In this work, experimental results are presented for varying count-rate and pulse shaping conditions. Using adaptive shaping, increased throughput is accepted while preserving the energy resolution observed using the longer shaping times.**

***Index Terms*—Digital signal processing, energy resolution, filters.**

I. Introduction

DIGITAL signal processing (DSP) is a rapidly expanding paradigm in the field of radiation spectroscopy. Advances in FPGAs make it possible to achieve an improved signal to noise ratio, higher throughput, reliability and flexibility as compared to traditional analog systems. Another advantage is the ability to implement adaptive shaping algorithms with flexibility to control the digital filter shaping parameters. In analog pulse processing, any adjustment in the shaping time constant perturbs the physical electrical circuits which makes adaptive pulse processing challenging in real time. Time-variant filters with an optimum signal to noise ratio can be realized in real-time using digital pulse processing. The concept of optimum signal processing using time variant filters and the digital techniques for real time pulse shaping in radiation measurements were previously explored in [1], [2], [3], [4], [5].

In this work, FPGA based real-time adaptive digital pulse shaping techniques are investigated for high count rate gamma-ray spectrometry applications with improved throughput and energy resolution. In digital pulse processing, the preamplifier output is sampled using a high-frequency digitizer. A digital S-K low pass filter is employed before the trapezoid-shaping filter to enhance the signal to noise ratio and to reduce baseline drifting in trapezoid shaping. A digital recursive trapezoid filter is used for pulse shaping to determine the pulse amplitude. The rate of rejection of piled up signal is reduced by adapting the trapezoid shaping parameters (rise time and flattop time) to the time interval between the adjacent preamplifier pulses. Digital pulse processing algorithms are implemented on the NI PXIe-7975R reconfigurable FPGA (Kintex-7) using the LabVIEW FPGA module. Simulations are performed using MATLAB to understand the effect of trapezoid shaping filter incorporating two decay constants on the trapezoid flattop, and baseline and energy resolution improvement after employing a digital Sallen-Key (S-K) filter. Experimental validation of the proposed adaptive digital pulse algorithms is performed using the digitized preamplifier signal of high-purity germanium detector using a ^{60}Co source by measuring the throughput and the resolution for different shaping times at various count rates.

II. Digital Signal Processing Algorithms

A conventional spectroscopy system uses a preamplifier, amplifier, and multi-channel analyzer (MCA) to obtain the pulse height distribution of the radiation source. These electronic components suffer from various issues such as,

Manuscript received July 1, 2016; revised xxxx xx, 2016. Current version published xxxx xx, xxxx.

The authors are with the Department of Nuclear Engineering, North Carolina State University, Raleigh, NC 27695 USA (e-mail: ssaxena@ncsu.edu; ayman.hawari@ncsu.edu).

Digital Object Identifier xxxx/TNS.2017.xxxxxx

electronic noise, dead time, ballistic deficit etc., which degrade spectroscopic performance. Alternatively, a digital pulse processing chain consists of a low pass filter, a digital recursive pulse shaping (e.g. trapezoidal) filter, a digital timing filter, a baseline restorer and a pile-up rejecter. This type of digital signal processing chain with an added adaptive capability for real-time implementation is discussed below.

A. Preamplifier Pulses of High Purity Germanium Detector

The high purity germanium (HPGe) output signal is a low-amplitude, short-duration current pulse. The preamplifier converts this current pulse to a voltage pulse whose amplitude is proportional to the energy deposited in the detector during a gamma-ray interaction. The HPGe preamplifier pulses exhibit a rapid rise time (~300 ns) and slow decay time (~55 μs). The preamplifier pulses can be mathematically represented as

$$f_{in}(t) = E\left(e^{-\frac{t}{\tau_F}} - e^{-\frac{t}{\tau_R}}\right), \quad (1)$$

where terms τ_F and τ_R are the decay time constant and rise time constant of the preamplifier pulse respectively. E is the height of the preamplifier pulse, which is proportional to the energy of incoming pulse. In this work, the detailed shape of the preamplifier pulse is shown in Fig. 1. As opposed to (1), it is observed that a typical preamplifier pulse of the HPGe detector is better described as consisting of two decay constants, a fast decay of short duration at the start of the decay and a slow decay for the remainder of the decay process. Thus, (1) is modified and can be expressed as

$$f_{in}(t) = E\left(e^{-\frac{t}{\tau_{F1}}} + e^{-\frac{t}{\tau_{F2}}} - e^{-\frac{t}{\tau_R}}\right), \quad (2)$$

where τ_{F1} and τ_{F2} are the two decay time constants and τ_R is the rise time constant of the preamplifier pulse. The z-transform representation of the signal after neglecting the rise time is given as

$$F_{in}(z) = E\left[\frac{z}{z-\beta_1} + \frac{z}{z-\beta_2}\right], \quad (3)$$

where $\beta_1 = e^{-\frac{\Delta t}{\tau_{F1}}}$, $\beta_2 = e^{-\frac{\Delta t}{\tau_{F2}}}$ and Δt is sampling time.

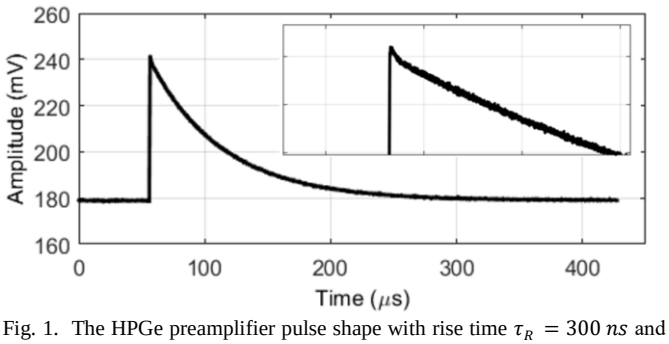

Fig. 1. The HPGe preamplifier pulse shape with rise time $\tau_R = 300\,ns$ and fall time $\tau_F = 55\,\mu s$. (inset shows the details of pulse shape).

B. Digital S-K Low Pass Filter

The digitized preamplifier is associated with white noise. In digital pulse shaping, the accumulation of noise causes baseline drifts in the shaped signal. Filtering the original preamplifier signal before shaping increases the signal to noise ratio (SNR) and reduces the baseline drifts in the shaped signal. The analog S-K filter is widely used in nuclear pulse processing which was proposed by R. P. Sallen and E. L. key in 1955. In reference [6], [7], it was shown that the digital S-K filter can be used to achieve high performance in signal processing. In this work, an S-K filter was implemented. The transfer function of digital S-K filter can be given as

$$F_{out}(z) = \frac{(f_{SK}(3-a_{SK}) + 2f_{SK}^2)F_{out}(z^{-1})}{1 + f_{SK}(3-a_{SK}) + f_{SK}^2} - \frac{f_{SK}^2 \times F_{out}(z^{-2}) + a_{SK}F_{in}(z)}{1 + f_{SK}(3-a_{SK}) + f_{SK}^2} \quad z > 0$$
$$F_{out}(z) = 0. \quad z \le 0 \quad (4)$$

The function F_{in} is the preamplifier signal and serves as an input to the digital S-K filter and F_{out} is the output of the S-K filter. The factor f_{SK} is the frequency filter factor, which adjusts the width of the output signal. a_{SK} is the amplitude filter factor. The block diagram of the digital S-K low pass filter is shown in Fig. 2.

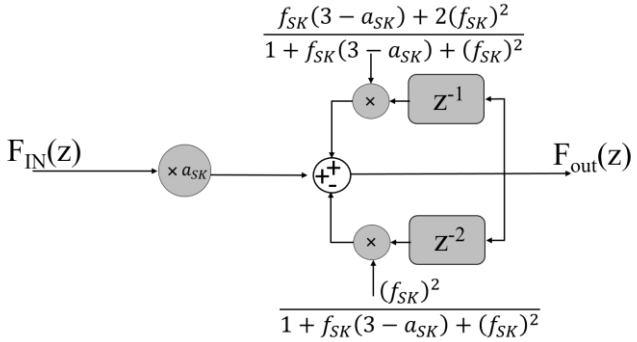

Fig. 2. A block diagram for the implementation of digital S-K low pass filter.

C. Digital Timing Filter

The RC-CR^2 filter is used for the generation of a bipolar waveform which can be used for various trigger generation. The transfer function of this filter can be expressed as,

$$F_{RC-CR2}(z) = \frac{z^{-1}(1-z^{-Avg})}{(1-z^{-1})} \times (1-z^{-R})^2 . \quad (5)$$

The parameter *Avg* represents a moving average in the time domain. The parameter R is equivalent to the rising edge of the preamplifier signal and is utilized in the first and second differentiation to generate the bipolar waveform. For the HPGe preamplifier pulses, R~200 ns − 300 ns. A CHECK window of width $2R$ (600 ns) is utilized that starts when the timing filter exceeds a certain threshold level *Th*. The value of threshold level *Th* is chosen such that it should eliminate the false trigger occurrences caused by noise. In addition, a zero-crossing detection (ZCD) logic searches for zero crossing within the CHECK window and if the zero crossing occurs, it will send a TRUE logic [8]. The ZCD triggers the determination of the trapezoid pulse height, which is proportional to the energy of incoming pulses. The pulse

height can be accurately determined at the start of trapezoid flattop at *A+B/4* point (see Fig. 3 below).

D. Digital Adaptive Shaping Filter

A pulse shaping algorithm is used to integrate the fast-rising preamplifier pulses and to differentiate the long tails. In this work, a digital trapezoid pulse-shaping algorithm is employed as the shaping filter. The digital shaping algorithm is set to be adaptive according to the time interval of separation between incoming preamplifier pulses. Based on the separation between the input pulses, it selects the optimum shaping parameters (the rise time and flattop time of the trapezoid shaping filter) for each incoming signal [9]. The potential advantages of the recursive trapezoid pulse shaping algorithms was explained in previous work [3], [4]. The flattop of the trapezoid filter can be adjusted to eliminate ballistic deficit. The most important advantage of trapezoid shaping is at high-count rate conditions where pile-up is a major consideration.

The trapezoid-shaping algorithm in discrete z transformation was discussed in [10], [11]. The trapezoid pulse can be synthesized as shown in Fig. 3 using the following equations

$$V_{TPZ}(t) = \sum_{i=1}^{4} V_i(t), \quad (6)$$

where V_{TPZ} is the function for trapezoid transformation. The trapezoid transmittance function can be obtained as,

$$V_{TPZ}(t) = \left(\frac{E}{t_1}\right) t - V_1(t-t_1) - V_1(t-t_2) - V_1(t-t_3),$$

$$V_{TPZ}(z) = \left(\frac{E}{A}\right)\left(1-z^{-A}\right)\left(1-z^{-(A+B)}\right)\frac{z^{-1}}{(1-z^{-1})^2}, \quad (7)$$

where A is the rise time and B is the flattop of trapezoid shaped pulse. The transfer function for the digital trapezoid filter can be given as,

$$H_{TPZ}(z) = \frac{V_{TPZ}(z)}{F_{IN}(z)}$$

$$H_{TPZ}(z) = \frac{1}{2A}\left(1-z^{-A}\right)\left(1-z^{-(A+B)}\right)\frac{z^{-1}(1-\beta_1 z^{-1})}{(1-z^{-1})^2}\frac{(1-\beta_2 z^{-1})}{(1-\frac{\beta_1+\beta_2}{2}z^{-1})} \quad (8)$$

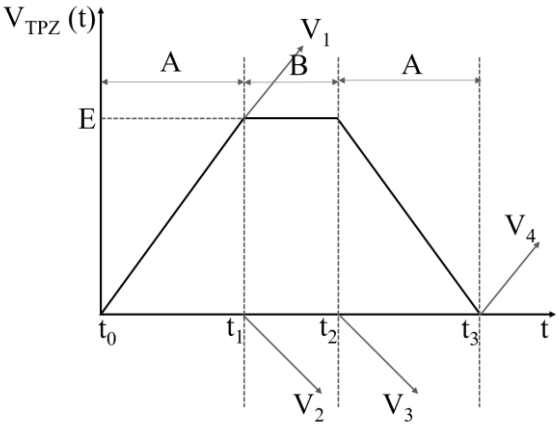

Fig. 3. Details of the synthesis of the trapezoid shaped pulse.

The block diagram of digital trapezoid shaping is shown in Fig. 4. The recursive digital trapezoid shaping algorithm is implemented in the MATLAB. Simulations are performed with the real HPGe preamplifier pulse of Fig. 1 with $\tau_R = 300\ ns, \tau_{F1}$= 600 ns and $\tau_{F2} = 55\ \mu s$. The simulation results are shown in Fig. 5. Conventionally, the recursive digital trapezoid-shaping algorithm was developed for the preamplifier pulses with single decay constant [3], [4]. The simulation was performed with the conventional algorithm and as can be observed in Fig. 5(a), the flattop of the trapezoid shaped pulse is distorted at the start of flattop. With the implementation of the modified trapezoid shaping incorporating two-decay constant for the HPGe preamplifier pulses, improvement in the trapezoid flattop is observed as shown in Fig. 5(b). This approach is key as it allows the extraction of pulse height information at the beginning of each pulse, which helps in reducing pile up and increasing throughput.

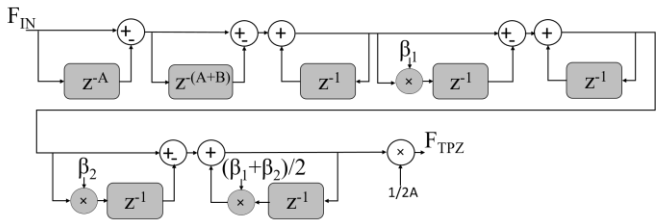

Fig. 4. Block diagram of the digital trapezoid-shaping algorithm.

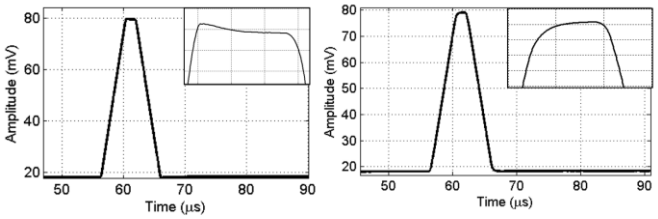

Fig. 5. Trapezoid shaping, (a) using the conventional algorithm, (b) using two decay constants for the input pulse (insets show the details of the pulse shape).

E. Digital Baseline Restoration

The preamplifier pulses of the HPGe detector contains bias due to detector leakage current, electronics etc. The trapezoid transformation of these preamplifier pulses does not eliminate the baseline shift. For the determination of actual trapezoid height, accurate baseline estimation is required. Baseline determination is realized by digital averaging of the trapezoid baseline with the gated restoration scheme. The fluctuations in baseline of the trapezoid shaped pulses are reduced by the use of a digital S-K low pass filter before the trapezoid transformation. When a preamplifier pulse arrives, ZCD will go high and the baseline gate will be open for the duration of the trapezoid width (*A*+*B*+*A*). In the case of pile-up, if any ZCD occurs within the trapezoid width, the baseline gate will remain open for another (*A*+*B*+*A*) duration. The baseline determination is performed by a moving average filter when the baseline gate is closed. In the signal processing chain, the trapezoid signal is digitally delayed to synchronize with the baseline trigger generation algorithm. The baseline value is triggered exactly at the start of the trapezoid shaped pulse and is subtracted from the trapezoid wave for the determination of

This article has been accepted for publication in a future issue of this journal, but has not been fully edited. Content may change prior to final publication. Citation information: DOI 10.1109/TNS.2017.2692219, IEEE Transactions on Nuclear Science

trapezoid height. The efficiency of baseline determination degrades with increasing count rate. This increases uncertainty in trapezoid height determination which further deteriorates the energy resolution at high count rates. The experimental results for energy resolution with input count rates are demonstrated in next section.

The digital S-K low pass filter is employed for elimination of high frequency noise. The simulation results for digital S-K filtration are shown in Fig. 6. The preamplifier pulses are generated at count rate of 10 kcps using Poisson interval distribution. All the pulses are characterized with identical height with different white noise components. The improvement in the baseline of trapezoid shaped pulses using S-K low pass filter is clear in Fig. 6(b). The improved baseline makes the digital baseline estimation more accurate, which will further improve the energy resolution.

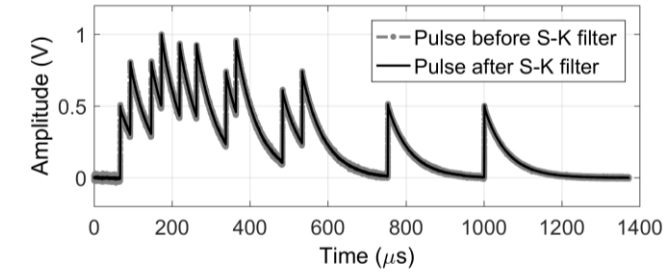

(a)

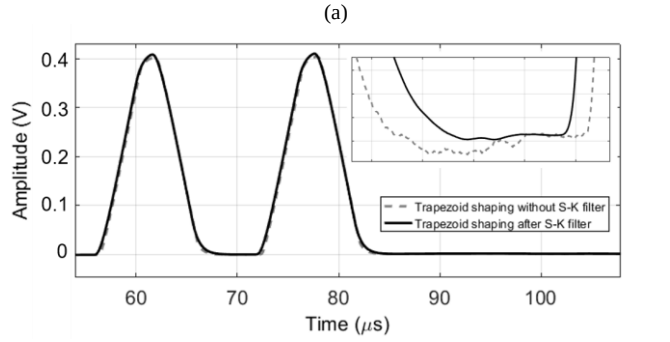

(b)

Fig. 6. (a) Simulated preamplifier pulses piled up at count rate of 10 kcps, SNR(original)=17.80 dB, after filtering using S-K low pass filter (f_{SK}=0.30, a_{SK}=0.051) SNR(S-K)=19.79 dB, (b) Trapezoid shaped pulses, inset shows improvement in the baseline between the two trapezoids using S-K filter.

F. Pile-up Rejection Algorithm

Preamplifier pulse rise time varies between 200 ns - 300 ns. As discussed previously, the timing filter is a CR-RC^2 filter. A CHECK window of width $2\tau_R$ starts when the timing filter crosses certain threshold (Th) to avoid false triggering (*Th*=100 mV). If there is no rising edge pile-up, zero crossing ocuurs within CHECK window1. In the case rising edge pile-up, the rise time of an incoming pulse increases and ZCD does not occur within CHECK window1. If the ZCD occurs after CHECK window1, and within CHECK window2, the pulse is treated as suffering from rising edge pile-up and is rejected.

In the case of trailing edge pile-up, at the zero crossing of the first incoming pulse, two pile-up windows of *A+B/4+P*

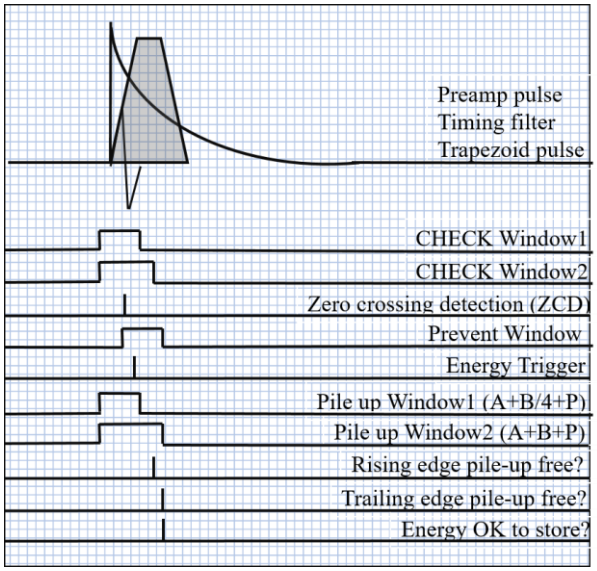

Fig. 7. Digital pulse processing sequential logic demonstrating various triggers and logic windows.

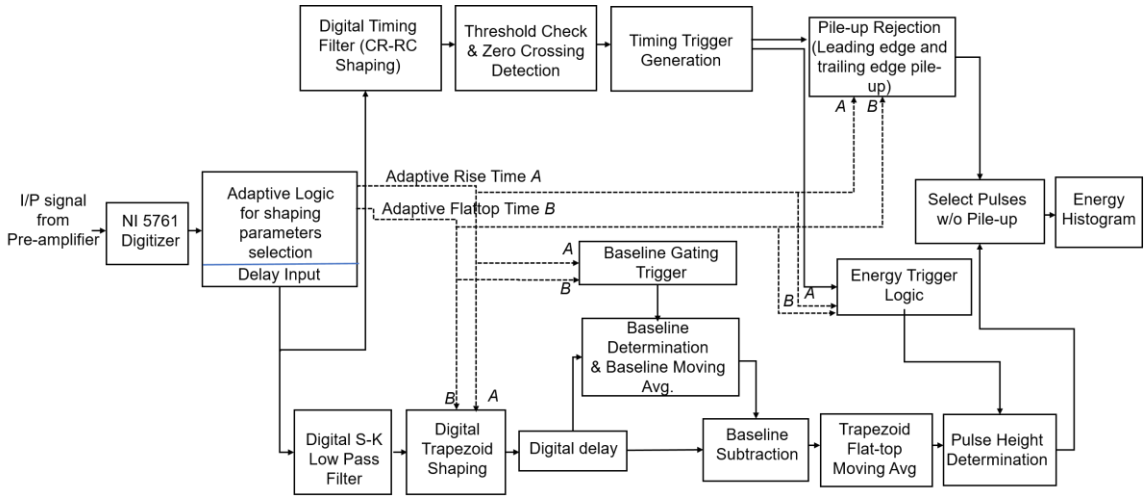

Fig. 8. A block diagram representing the adaptive digital pulse processing chain.

and *A+B+P* will be started that will look for any other zero crossing (ZCD) within that window. If a second pulse comes within the *A+B/4+P* window, both the pulses will be rejected. If no ZCD occurs within *A+B/4+P* and it occurs between *A+B+P*, the energy of the first pulse will be accurately latched, pile up logic will send a true pulse to store the first pulse energy value and the second pulse will be discarded. Two pile-up check triggers are used for the pile-up rejection: rising edge pile-up, trailing edge pile-up. If both of the triggers are TRUE, then only pulse height information will be included in the pulse height spectrum. The sequence of the digital pulse processing approach is schematically represented in Fig. 7 and in the block diagram is shown in Fig. 8.

III. Experimental Implementation

The DSP system testing configuration is shown in Fig. 9. A 380 µCi ^{60}Co gamma source is used for testing the performance of the system. The source position is varied to obtain different count rates. The measurements are carried out using a coaxial P-type Ortec GEM series coaxial HPGe detector having a relative efficiency of 25% at 1333 keV with a reset preamplifier. The high voltage provided to the detector element is +4800 V.

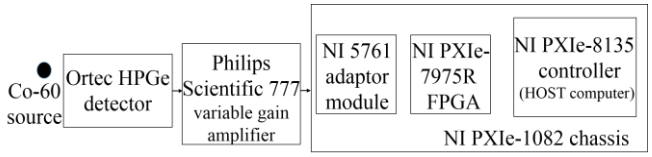

Fig. 9. A block diagram representing the system configuration for digital pulse processing.

The HPGe detector's preamplifier signal is digitized using the National Instruments (NI) adaptor module NI 5761, which is a 14 bit, 4-channel digitizer with a bandwidth of 500 MHz and sampling rate of 250 MS/s. The digitized preamplifier signals are fed to the reconfigurable NI PXIe-7975, which has the Xilinx FPGA Kintex-7 XC7K410T. The DSP algorithms are implemented using LabVIEW FPGA 2014 module. This module interfaces with the adaptor module and has a hardware description language (HDL) integration capability. The Xilinx Vivado 2013.4 compilation tool is used for the compilation of the LabVIEW FPGA Virtual Instrument (VI). The HOST VI communicates with the LabVIEW FPGA VI to display the various pulse shapes. The FPGA device utilization is tabulated in Table 1.

TABLE I
FPGA Device Utilization

Device Utilization	Used	Total	Percent
Total slices	21846	63550	34.4
Slice registers	56884	508400	11.2
Slice LUTs	53780	254200	21.2
Block RAMs	200	795	25.2
DSP48s	17	1540	1.1

Representative ^{60}Co energy spectra recorded using the adaptive DSP system at count rates of 10 kcps, 50 kcps and 100 kcps are shown in Fig. 10. The measured FWHM for 1333 keV peak is 1.86 keV, 2.04 keV and 2.09 keV at 10 kcps, 50 kcps and 100 kcps respectively with adaptive shaping times.

The full width half maximum (FWHM) versus the rise time plot for different flattop times is shown in Fig. 11. The resolution performance is consistent until a 2 µs shaping time with the digital system while resolution starts deteriorating with analog system for if shaping time is reduced below 6 µs. The rise time of the digital trapezoid filter is equivalent to the shaping time of analog systems. In further discussion, the rise time of the digital pulse processing system is referred to as shaping time.

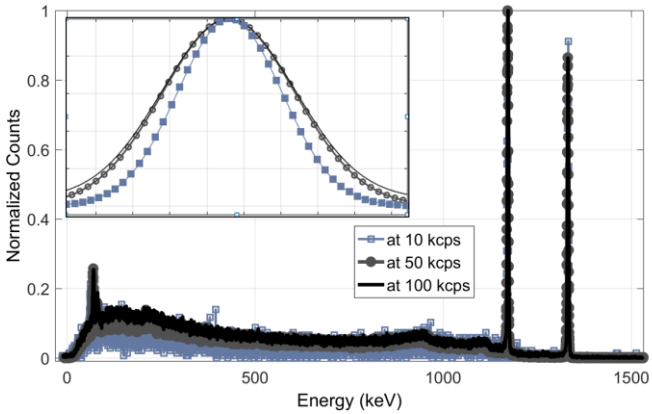

Fig. 10. The ^{60}Co energy spectrum recorded using DSP system at count rates of 10 kcps, 50 kcps and 100 kcps with measured FWHM for 1333 keV peak is 1.86 keV, 2.04 keV and 2.09 keV respectively with adaptive shaping times (insets show the detailed 1333 keV peak shape).

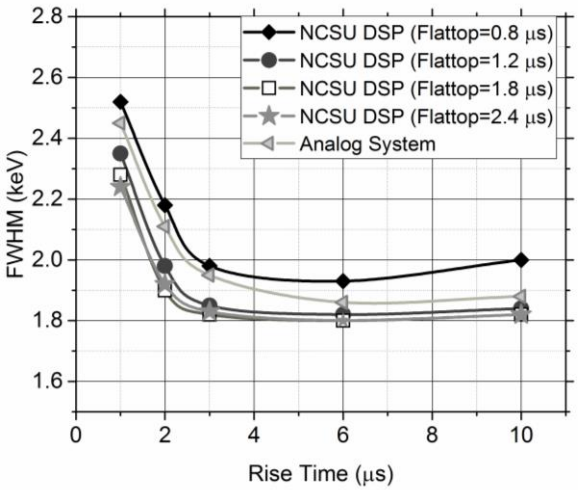

Fig. 11. FWHM versus rise time for many flat top times of 1333 keV ^{60}Co peak at count rate of 1 kcps.

The results of FWHM versus input count rate (ICR) for various shaping times for the analog and digital system are shown in Fig. 12 (a). The close proximity in time between two consecutive pulses results in an increase in the shot noise, and uncertainty in the baseline determination which degrades the energy resolution at high-count rates [12]. The plot of throughput versus ICR is shown in Fig. 12(b), which compares

the throughput performance of the adaptive digital pulse shaping to the digital shaping with fixed shaping time as well as to analog signal processing. Using adaptive digital pulse processing, throughput performance is comparable to a 1 μs shaping time but with an improved resolution similar to that achieved by using longer shaping times.

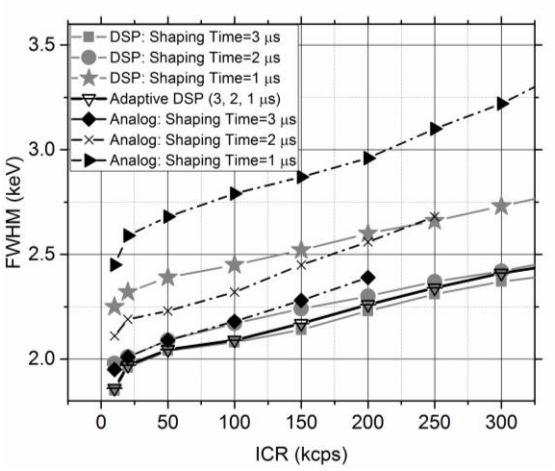

(a)

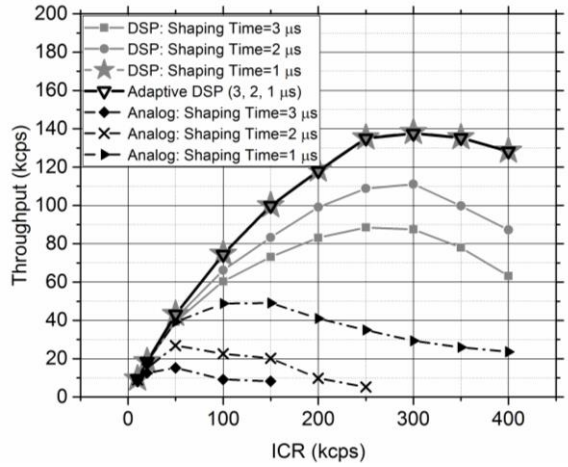

(b)

Fig. 12. (a) FWHM at 1333 keV ^{60}Co peak versus input count rate (ICR) for different shaping times, (b) Throughput versus input count rate (ICR) for different shaping times.

Fig. 13 shows the throughput performance of the adaptive digital pulse processing including the distribution the number of pulses shaped with a given shaping time in comparison to theoretical calculations using the exponential model of the distribution of time intervals [13].

In this model, the probability of the next event taking place in an interval dt after a delay of Δt can be approximated as $r \times e^{-r\Delta t}$, where r is the input count rate. The fraction of events occurring in a particular time interval (Δt) is calculated as $1 - e^{-r\Delta t}$, where Δt is the shaping time in this calculation. As it can be seen in Fig. 13, the distribution of number of pulses shaped with different shaping times using adaptive digital pulse processing is in good agreement with theoretical calculations. This provides reasonable validity to the observed performance of the adaptive DSP system.

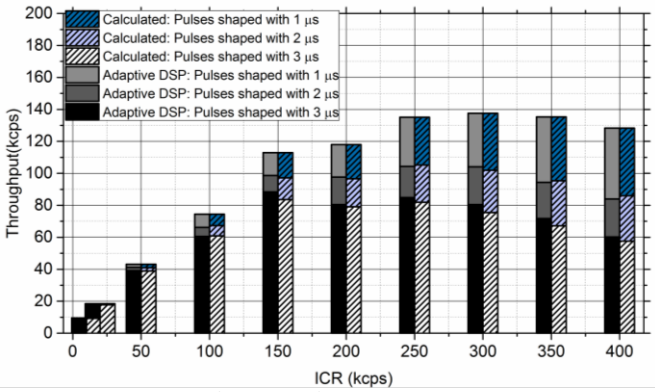

Fig. 13. Throughput performance of adaptive digital pulse processing with distribution of pulses shaped with different shaping times in comparison to theoretical calculation.

IV. Conclusion

This work illustrates the implementation of real-time adaptive digital pulse shaping, based on a trapezoid filter, in gamma-ray spectrometry applications using an HPGe detector. It was found that a digital trapezoid filter algorithm incorporating two decay constants to describe the HPGe preamplifier pulse improves the trapezoid flattop. This allows the extraction of the pulse height information at the beginning of each pulse, which limits pulse pile-up effects. Consequently, it is possible to perform real-time selection of the shaping parameters (rise time and flattop time of the trapezoid shaping filter) for each incoming signal based on the time separation from a subsequent pulse. Experimental testing of the developed adaptive approach demonstarted that higher throughput is achievable while preserving the energy resolution observed using longer shaping times.

Acknowledgment

This work was partially supported by a US Department of Energy Nuclear Energy University Program reactor infrastructure grant.

References

[1] M. Bertolaccini, C. Bussolati, S. Cova, I. De Lotto, E. Gatti. (1968, April). Optimum processing for amplitude distribution evaluation of a sequence of randomly spaced pulses. *Nuclear Instruments and Methods* [online]. *Vol. 61, Issue 1,* pp. 84-88. Available: http://www.sciencedirect.com/science/article/pii/0029554X68904539

[2] H. Koeman. (1975, Jan.). Discussion on optimum filtering in nuclear radiation spectrometers. *Nuclear Instruments and Methods* [online]. *Volume 123, Issue 1,* pp. 161-167. Available: http://www.sciencedirect.com/science/article/pii/0029554X75900919

[3] V. T. Jordanov, G. F. Knoll. (1994, June). Digital synthesis of pulse shapes in real time in high resolution radiation spectroscopy. *Nuclear Instruments and Methods in Physics Research Section A: Accelerators, Spectrometers, Detectors and Associated Equipment* [online]. *Volume 345, Issue 2,* pp. 337-345. Available: http://www.sciencedirect.com/science/article/pii/0168900294910111

[4] V. T. Jordanov, G. F. Knoll, A. C. Huber, J. A. Pantazis. (1994). Digital techniques for real time pulse shaping in radiation measurements. *Nuclear Instruments and Methods in Physics Research* [online]. *A 353,* pp. 261-264. Available:

https://deepblue.lib.umich.edu/bitstream/handle/2027.42/31113/0000009.pdf?sequence=1

[5] A. Geraci, A. Di Odoardo, S. Riboldi, G. Ripamonti. (2000, Dec.). Adaptive digital spectroscopy in programmable logic. *IEEE Transactions on Nuclear Science* [online]. *Vol. 47, No. 6*, pp. 2765-2772. Available: http://ieeexplore.ieee.org/xpl/abstractAuthors.jsp?arnumber=901184

[6] J. Zhou, X. Hong. (2013, Jan.). Improvement of digital S-K filter and its application in nuclear signal processing. *Nuclear Science and Techniques* [online]. *24, 060401*, pp. 1-7. Available: http://www.j.sinap.ac.cn/nst/EN/abstract/abstract405.shtml

[7] X. Hong et al. (2015). New methods to remove baseline drift in trapezoidal pulse shaping. *Nuclear Science and Techniques* [online]. *26, 050402*, pp. 1-5. Available: http://www.j.sinap.ac.cn/nst/EN/abstract/abstract629.shtml

[8] S. Saxena, M. Liu, A. I. Hawari. (2015, Nov.). Implementation of an FPGA-based digital coincidence Doppler broadening spectrometer for PAS measurements. *Transactions of American Nuclear Society*. *113, 86* pp. 486-488.

[9] A. Abba, A. Geraci. (2012, Oct.). Dynamic maximization of filter length in digital spectroscopy. *IEEE Transactions on Nuclear Science* [online]. *Vol. 59, No. 5*, pp. 2451-2456. Available: http://ieeexplore.ieee.org/xpls/abs_all.jsp?arnumber=6265349

[10] C. Imperiale, A. Imperiale. (2001, July). On nuclear spectroscopy pulses digital shaping and processing. *Measurement* [online]. *Vol. 30, Issue 1*, pp. 49-73. Available: http://www.sciencedirect.com/science/article/pii/S0263224100000579

[11] Z. Guzik, T. Krakowski. (2013, May). Algorithms for digital γ-ray spectroscopy. *Nukleonika* [online]. *58(2)*, pp. 333-338. Available: http://www.ichtj.waw.pl/nukleonika/www/back/full/vol58_2013/v58n2p333f.pdf

[12] M. O. Deighton. (1972, Aug.). Analysis of pulse-rate dependent noise and counting losses in active processor with fast recovery. *Nuclear Instruments and Methods* [online]. *Vol. 103, Issue 1*, pp. 1-12. Available: http://www.sciencedirect.com/science/article/pii/0029554X72904521

[13] G. F. Knoll, "Radiation detection and measurement," 4th ed., John Wiley & Sons, Inc., 2010, pp. 99-102.